Geophys. J. Int. (1998) **135,** 375–387

Tests of glacial rebound models for Fennoscandinavia based on instrumented sea- and lake-level records

Kurt Lambeck,[1] Catherine Smither[1] and Martin Ekman[2]

[1] *Research School of Earth Sciences, The Australian National University, Canberra,* ACT 0200, *Australia. E-mail: Kurt.Lambeck@anu.edu.au*
[2] *Geodetic Research Division, National Land Survey,* SE-801 82 *Gävle, Sweden*

Accepted 1998 May 29. Received 1998 May 20; in original form 1998 February 24

SUMMARY

Evidence for changing sea levels in northwestern Europe related to glacial rebound is found in both the geological record of the past millennia and in the instrumental records of the past two centuries. The latter records are of two types: records of sea-level change, primarily from the Baltic and the Gulfs of Finland and Bothnia, and records of the tilting of some of the larger lakes in both Finland and Sweden. The sea-level records are particularly important because of their long duration and high quality, their large number and good spatial distribution, and the spatially coherent background noise. The two instrumental data types are complementary and provide constraints on the upper-mantle rheology and on the distribution of ice during the late glacial stage. Comparisons of the observed rates of change of the water levels with models for glacial rebound yield earth models with a lithospheric thickness of 80–100 km and an upper-mantle viscosity of $(4–5) \times 10^{20}$ Pa s, effective parameters that are consistent with those obtained from the analysis of the geological evidence for the same region. The mareograph results support ice-sheet models in which the Late Weichselian ice thickness over the eastern and southern parts of Fennoscandia is relatively thinner than that for the western region, also consistent with the interpretation of the geological evidence for sea-level change. In addition, the instrumental records provide constraints on the eustatic sea-level change for about the past 100 years. A satisfactory separation of the earth rheology parameters from this rate of change can be achieved by estimating the latter only from those records for which the predicted isostatic effects are small. A check on these results is possible by using the lake-level records to establish constraints on the earth-model parameters and the sea-level records to constrain also the eustatic change. All approaches lead to an average eustatic sea-level rise for the past century of about 1.1 ± 0.2 mm yr^{-1}.

Key words: mareographs, postglacial rebound, sea-level change, tide-gauges.

1 INTRODUCTION

Glacial rebound models are usually based on geological indicators of sea-level change. The advantage of these records is that they extend back to the time of deglaciation and sometimes, for areas outside the limits of former glaciation, back to the time of maximum glaciation. Their disadvantage is that the observations are of relatively low accuracy and are frequently inhomogeneous in their nature. Questions about the relationship between the shoreline indicators and mean sea level may also add to the uncertainty. Complementary information on the time dependence of the position of sea level relative to the crust is available from tide gauge or mareograph observations. The advantage of these records is that the estimates of present sea-level change are of a relatively high precision and homogeneity. Their disadvantage is that the record is short, corresponding to the tail-end of the deglaciation signal, and influenced by other, higher-frequency, signals.

In the case of Scandinavia, the mareograph records are important for several reasons.

(1) There is a good spatial distribution of records around the Gulfs of Bothnia and Finland, the Baltic proper and its connection to the North Sea, and the Norwegian Atlantic coast. The records for the northern end of the Gulf of Bothnia and for the southern Baltic shoreline are particularly important because geological evidence for these regions is generally sparse (see Figs 1 and 2 of Lambeck *et al.* 1998; hereafter referred to as Paper I).

(2) The records extend further back in time than is often the case for instruments of this kind, with some 50 sites having records that span at least 60 years and, for about one-half of them, 100 years.

(3) The Baltic Sea with its two adjoining gulfs is essentially free from astronomical tides and most other short-period variations, so that the 'short-term' noise levels of the mareograph records are relatively low.

(4) The good coherence of long-period signals in the sea levels of the Baltic Sea, including the two gulfs, means that analysis methods can be used that reduce the impact of any longer-period fluctuations on estimates of the secular trends (Ekman 1996a). Together, these factors mean that the precision with which secular trends can be extracted from the records is considerably better than is usual for tide-gauge records.

No geodetic data have been used to constrain the earth and ice models derived in Paper I, and the objective of the present paper is twofold: (1) to use this independent data to test the model and determine whether improvements to it can be made using the instrumental record; and (2) to obtain estimates of the recent secular change in global sea level for the past 100 years by subtracting the model-predicted isostatic contributions from these high-quality records.

2 THE MAREOGRAPH RECORDS OF FENNOSCANDIA

A consistent computation of present rates of glacial rebound, based on sea-level records from the whole of Fennoscandia, has been performed by Ekman (1996a). The sea-level stations used include 56 stations in the Baltic Sea and adjacent waters, i.e. along the coasts of Finland, Sweden, Norway, Denmark, Germany, Poland, the Baltic countries, and part of Russia. These stations have reliable records spanning 60 years or more, with one station record, Stockholm, spanning about 200 years (Ekman 1988). The relative uplift rates (and their standard errors) have been estimated from the linear regression of annual means of sea level recorded at these sites and corrected for the 18.6 year lunar nodal tide using the equilibrium-tide assumption. The results are reproduced in Table 1 and further information is given by Ekman (1996a). Estimates of secular change range from close to 9 mm yr^{-1} in the northern part of the Gulf of Bothnia to -1 mm yr^{-1} at the southern coast of the Baltic proper. (Positive rates mean that the rate of land uplift exceeds the rate of sea-level rise so that sea level appears to be falling, a sign convention that is consistent with that usually used in the analysis of the geological evidence.)

In order to compare estimates from the various sites with each other, these rates must refer to a common time period so as to eliminate the effects of long-period climatic-change-induced fluctuations. The standard period adopted in the above computation is the 100 year period 1892–1991, a period that is common for many stations and which avoids high- and low-water years at the two ends of the period. Because long-term sea-level variability across the Baltic Sea, on a time scale longer than one month, shows a very considerable coherence (Samuelsson & Stigebrandt 1996), every sea-level station not containing these years has been reduced to the standard period by a differential comparison with a reference station for the interval of the deviating record. That is, if the record length at station A deviates from the prescribed 100 year interval, this record is compared with the reference station record R for the same period to obtain the differential secular rate between A and R for this interval. The secular rate for A for the 100 year interval is then the rate at R for this time plus the differential rate for the deviating interval. If part of the deviating record is missing, then the reference record does not include data corresponding to these missing years either when estimating the differential secular rate. The station adopted as the principal reference station is Stockholm, since it is situated close to the middle of the Baltic Sea and has the longest record, covering the years of all the other stations. Although the level of the Baltic is correlated with the level outside it, the coherence weakens when one reaches the transition area between the Baltic and North seas, and the station Smögen (north of Göteborg) serves as the reference station for the non-Baltic mareographs. The coherence of the extra-Baltic records is generally good.

The standard error of a secular rate is typically 0.2 mm yr^{-1}, ranging from 0.1 mm yr^{-1} at the Baltic entrance to between 0.2 and 0.3 mm yr^{-1} in the innermost parts of the gulfs of Bothnia and Finland (Ekman 1996b). The main reason for this spatial variability in variance is the wind-driven pumping of North Sea water into or out of the Baltic Sea, especially during winters (Ekman 1997). Because of the strong correlation between sea-level fluctuations at the Baltic sites, the standard error of the differential uplift rate between two mareographs is usually smaller, but dependent on their relative positions. Thus two mareographs within the Baltic Sea will yield a standard error for the differential uplift rate of about 0.1 mm yr^{-1}, while the same estimate for Norwegian Sea and Gulf of Bothnia sites is about 0.3 mm yr^{-1}. In the following, a conservative upper limit of 0.3 mm yr^{-1} has been used for the standard errors of all uplift rates. This value is consistent with the differences in estimated rates between the analysis by Ekman and that by Vermeer *et al.* (1988) using a different adjustment procedure.

In addition to the sea-level monitors, lake levels have been monitored in Sweden and Finland, and in some cases long records exist in pairs for the larger lakes (e.g. Sirén 1951). These observations can likewise be used as independent tests of the rebound models, with their advantage over the coastal sites being that the observations are from localities within the interior of the land mass and hence increase the spatial variability of the present rebound information. Four such lakes have provided particularly useful records, two in southern-central Sweden and two in southern Finland. Table 2 summarizes the results based on the analysis by Ekman (1996a) of the original records. The distance between the pair of lake-level stations is around 100 km, and the record lengths are close to 100 years. The results give an uplift gradient close to 1 mm yr^{-1} per 100 km, in good accordance with the gradients inferred from nearby coastal sites. The standard deviations of these differential rates are conservatively estimated at 0.2 mm yr^{-1}.

3 NUMERICAL MODEL RESULTS

3.1 Glacial rebound models of sea- and lake-level change

3.1.1 Earth rheology and ice-sheet models

The glacial rebound and sea-level change models used here have been discussed in detail in Paper I. The range of earth

Table 1. Summary of observed and predicted rates of present crustal uplift and residuals for selected models. The observed values (column 4) are from Ekman (1996a). The residuals $\varepsilon^0(\varphi)$ correspond to three solutions: (i) the earth-ice model based on the geological data, (ii) the solution (8) for the ice model SCAN-1, and (iii) the solution (11) for the ice model SCAN-2.

Site	Latitude	Longitude	Observed rate (mm yr^{-1})	Residuals (mm yr^{-1}) (i)	(ii)	(iii)
Århus	56.15	10.22	−0.49	0.01	0.38	0.10
Bergen	60.40	5.30	0.24	−0.79	0.26	−0.16
Björn	60.63	17.97	5.95	0.32	0.22	0.01
Degerby (Åland)	60.03	20.38	4.11	0.06	−0.75	−0.31
Draghällan	62.33	17.47	7.57	0.68	0.90	0.13
Esbjerg	55.47	8.45	−1.04	0.13	0.51	0.42
Fredericia	55.57	9.77	−0.96	−0.09	0.20	0.14
Frederikshavn	57.43	10.57	0.49	−0.34	0.58	−0.34
Furuögrund	64.92	21.23	8.75	1.27	0.74	0.74
Gävle	60.68	17.17	5.90	0.08	0.37	−0.18
Gedser	54.57	11.97	−0.94	−0.25	−0.25	0.28
Grönskär	59.27	19.03	3.97	0.38	−0.12	0.14
Hamina	60.57	27.18	1.67	−0.52	−1.24	−0.48
Hanko	59.82	22.97	2.99	0.26	−0.68	0.00
Heimsjø	63.43	9.07	1.47	−0.62	1.29	−0.95
Helsinki	60.15	24.97	2.28	−0.13	−0.97	−0.25
Hirtshals	57.60	9.95	0.38	−0.48	0.50	−0.45
Hornbæk	56.10	12.47	−0.08	−0.08	−0.01	0.07
Kaskinen	62.38	21.22	7.11	1.14	0.36	0.36
Kemi	65.73	24.55	7.14	0.56	0.15	−0.13
Klagshamn	55.52	12.97	−0.04	0.19	0.01	0.52
København	55.68	12.60	−0.24	−0.02	−0.10	0.25
Kolberg	54.18	15.57	−0.95	−0.52	−0.78	0.16
Korsør	55.33	11.13	−0.61	0.05	0.15	0.36
Kronstadt	59.98	29.78	0.09	−1.02	−1.72	−0.62
Kungsholmsfort	56.10	15.58	0.20	−0.28	−0.85	0.03
Landsort	58.75	17.87	3.06	−0.16	−0.32	−0.31
Lemström (Åland)	60.10	20.02	4.57	0.28	−0.47	−0.08
Liepaja	56.53	20.98	−0.30	−0.66	−1.43	−0.30
Lypyrtti	60.60	21.23	5.06	0.76	−0.09	0.30
Mäntyluoto	61.60	21.48	6.31	1.13	0.35	0.49
Marienleuchte	54.50	11.25	−0.72	0.08	0.19	0.62
Narvik	68.43	17.42	3.06	−0.13	1.21	0.43
Nevlunghavn	58.97	9.88	1.56	−1.23	0.38	−0.87
Ölands norra udde	57.37	17.10	1.29	−0.34	−0.74	−0.27
Oslo	59.90	10.75	4.10	−0.11	1.91	0.31
Oulu	65.03	25.43	6.66	0.52	−0.02	−0.33
Pietarsaari	63.70	22.70	8.04	1.57	0.72	0.72
Pillau	54.65	19.90	−1.22	−0.86	−1.07	−0.17
Raahe	64.70	24.50	7.54	1.14	0.40	0.30
Ratan	64.00	20.97	8.16	0.98	0.28	0.22
Rauma	61.13	21.48	5.22	0.49	−0.32	−0.07
Slipshavn	55.28	10.83	−0.83	−0.09	0.05	0.23
Smögen	58.37	11.22	1.99	−0.34	1.10	−0.23
Södertälje	59.20	17.63	3.66	−0.22	−0.19	−0.38
Stavanger	58.97	5.73	−0.19	−0.71	0.19	−0.28
Stockholm	59.32	18.08	3.98	0.05	−0.10	−0.15
Swinemünde	53.92	14.27	−0.77	−0.21	−0.29	0.49
Travemünde	53.97	10.87	−1.80	−0.93	−0.68	−0.27
Tregde	58.00	7.57	−0.05	−0.49	0.43	−0.30
Turku	60.42	22.10	4.05	0.35	−0.50	−0.06
Vaasa	63.10	21.57	7.62	1.21	0.41	0.37
Varberg	57.10	12.22	0.77	−0.07	0.56	−0.09
Vardø	70.33	31.10	0.81	−0.25	1.26	−0.17
Visby (Gotland)	57.65	18.30	1.45	−0.31	−0.91	−0.31
Warnemünde	54.18	12.08	−1.06	−0.33	−0.28	0.29
Wismar	53.90	11.47	−1.31	−0.50	−0.30	0.17
Ystad	55.42	13.82	−0.62	−0.48	−0.85	−0.09

Table 2. Summary of observed and predicted differential uplift rates for pairs of lake-level stations. The observed values are from Ekman (1996a). The predicted differential uplift rates correspond to three solutions: (i) the earth-ice model based on the geological data, (ii) the solution (10) for the ice model SCAN-1, and (iii) the solution (12) for the ice model SCAN-2.

Lake	Sites	Observed diff. uplift (mm yr^{-1})	Predicted diff. uplift (mm yr^{-1})		
			(i)	(ii)	(iii)
Vänern	Sjötorp/Vänersborg	0.74	0.86	1.21	1.32
Vättern	Motala/Jönköping	1.62	1.12	1.16	1.21
Päijänne	Haapakoski/Kalkkinen	1.08	0.96	1.03	1.09
Saimaa	Juurisalmi Lauritsalla^{-1}	0.64	0.57	0.70	0.68

models explored is restricted to three-layered models defined by three parameters: an effective lithospheric thickness H_1 and the effective viscosities for the upper and lower mantle ($\eta_{\rm um}$, $\eta_{\rm lm}$), with the division between the two zones occurring at a depth of 670 km corresponding to a major seismic discontinuity observed at that depth. The models are gravitationally consistent, the earth is compressible, and the density and elasticity are defined by realistic parameters inferred from seismic data. Lateral homogeneity in the earth response is assumed. The contributions to sea-level change from the distant ice sheets are included, as is the contribution from the changing sea level itself as mass is exchanged between the continental-based ice and the oceans. The relative sea-level change prediction includes the crustal rebound and geoidal change contributions.

A major uncertainty in modelling the glacial rebound is the geometry of the ice load, particularly from the time of the maximum glaciation to the end of deglaciation. Two models are considered. The first, based on the ice retreat contours of Andersen (1981) and Pedersen (1995) and on the ice thickness estimates of Denton & Hughes (1981), is largely independent of the choice of earth-model parameters. The ice profiles are described as quasi-parabolic functions (*cf.* Paterson 1969), based on the assumption that the ice sheet is frozen to its base. The maximum ice thickness occurring in this model is about 3400 m centred over the Gulf of Bothnia and northern Finland. This thickness is ice-model-dependent, but it is also one of the parameters that can be inferred from the comparison of model predictions with observations of shoreline age–height relations. Earlier studies have indicated that this maximum value for the ice thickness is excessive (Lambeck *et al.* 1990), and the average scaling value of 0.62, inferred from the comparisons with the geological data, is adopted here (Paper I). This scaled ice model is referred to as SCAN-1. However, rebound models based on this ice sheet, irrespective of the earth-rheology parameters, yielded discrepancies between geological observations and predictions that exhibited a considerable spatial variability and which are indicative of a need to modify the ice model beyond what can be done with the single scaling parameter. In particular, the evaluation of the discrepancies led to the conclusion that the parabolic profile assumption for the ice sheet is inappropriate for the eastern and southern regions; that is, the ice height there increased much more slowly with distance in from the ice margin than is assumed to be the case when the parabolic profiles are adopted. This produced the second model (SCAN-2), characterized by parabolic profiles in the west but by profiles for the east and south that exhibit smaller gradients with distance inwards from the ice margin. This model is generally consistent with the ice sheet being cold-based over Norway and the high ground of Sweden and warm-based over Finland, the Baltic Sea and northern Europe (e.g. Kleman *et al.* 1997).

3.1.2 *Models for sea-level change*

The observation equation for the sea-level monitor at a position ϕ is

$$\Delta\dot\zeta^{\rm o}(\phi)=\Delta\dot\zeta^{\rm p}(\phi, E_k, I_j)+\Delta\dot\zeta^{\rm e}+\varepsilon^{\rm o}(\phi), \qquad k=1,\dots K; j=1\dots J, \tag{1}$$

where $\Delta\dot\zeta^{\rm o}$ is the observed change and $\Delta\dot\zeta^{\rm p}$ is the predicted change for earth-model E_k and ice model I_j. $\varepsilon^{\rm o}(\phi)$ is the correction to the observed rate at position ϕ, and $\Delta\dot\zeta^{\rm e}$ is the eustatic sea-level change, being constant by definition over the area. (To be consistent with the geological models, $\Delta\dot\zeta^{\rm e}$ is negative if sea levels in the past lie below present mean sea level, corresponding to an increasing ocean-volume environment.) The earth-model parameters H_1, $\eta_{\rm um}$, $\eta_{\rm lm}$ are contained within $\Delta\dot\zeta^{\rm p}(\phi, E_k, I_j)$. The estimate of the eustatic sea-level change follows from (1) as

$$\Delta\dot\zeta^{\rm e}=\sum_m\left[(\Delta\dot\zeta^{\rm o}_m-\Delta\dot\zeta^{\rm p}_m)/\sigma_m^2\right]\Big/\sum_m\sigma_m^{-2}, \qquad m=1,\dots M, \tag{2}$$

where σ_m is the standard deviation of the observed rate of the mth observation. A value of $\sigma_m=0.3$ mm yr^{-1} is assumed for all sites (see above). For earth model E_k, the measure of fit to the observed rates is defined as

$$\Psi_k^2=\frac{1}{M}\sum_m\left[\frac{\Delta\dot\zeta^{\rm o}_m-\Delta\dot\zeta^{\rm p}_m(E_k)-\Delta\dot\zeta^{\rm e}}{\sigma_m}\right]^2. \tag{3}$$

As in Paper I, broad limits to the permissible model space are defined, and parameters E_{k*} within this space are sought that lead to the minimum value for Ψ_k^2. Then, if the rebound model is correct, the estimates for σ_m are realistic, and there are no other contributions to the sea-level change other than a secular eustatic rate, the expected value of the dimensionless quantity Ψ_k^2 is unity.

The estimate of accuracy of the model parameters for the solution corresponding to this least-variance model E_{k*} is given by the statistic (*cf.* Paper I)

$$\Phi_k^2=\frac{1}{M}\sum_m\left[\frac{(\Delta\dot\zeta^{{\rm p},k}_m+\Delta\dot\zeta^{{\rm e},k})-(\Delta\dot\zeta^{{\rm p},k*}_m+\Delta\dot\zeta^{{\rm e},k*})}{\sigma_m}\right]^2. \tag{4}$$

$\Delta\dot\zeta^{{\rm p},k}_m+\Delta\dot\zeta^{{\rm e},k}$ is the predicted rate, at observation site m, of the relative sea-level change for any earth model E_k, and includes the estimate of the eustatic rate corresponding to that particular earth model. $\Delta\dot\zeta^{{\rm p},k*}_m+\Delta\dot\zeta^{{\rm e},k*}$ is the rate for the model E_{k*} that leads to the least-variance solution and includes the estimate of the eustatic change for that particular model. Models for which $\Phi_k^2\le r$ differ from the best-fitting model by an amount equal to or less than r times the average observational variance of the data. Because the σ_m estimates may have already been overestimated by about 50 per cent (see above), the criterion $\Phi_k^2=1.78$ is used below to specify the accuracy of the earth-model parameters. This, in terms of original observational accuracies of about 0.15 mm yr^{-1}, corresponds to the 90 per cent confidence limit.

A potentially unsatisfactory aspect of the formulation (1)–(3) is that any long-wavelength limitations in the model can lead to misleading results for the estimate of the secular rate $\Delta\dot{\zeta}^{e}$. An alternative approach would be to assume that the eustatic rate is known from global analyses of tide gauges and to impose this upon the model. The difficulty with this is that this rate is not well constrained because all tide-gauge records are contaminated to varying degrees by non-eustatic factors, and few of the global records are of the same duration or quality as the Baltic data. A second approach is to estimate where a particular rebound model predicts a zero rate for the glacio-isostatic sea-level change and to use the mareograph record from sites on or close to this contour to estimate the rate of eustatic sea level and to impose this value on (1). The estimate of the secular rate is then given by (3), but with the summation carried out only for the subset of sites (M') for which

$$\Delta\dot{\zeta}^{p}_{m'} = 0 \pm \sigma_{m'}, \qquad m' = 1, \ldots M'. \tag{5}$$

3.1.3 *Models for lake-level change*

The lake-level observations consist of time series of the differences in the levels at two locations, and the rate of change of this difference establishes the rate of tilting of the crust or, equivalently, the differential rate of uplift at the two locations. Comparison of these observations with model predictions are made in a similar manner as before: for earth model E_k, the differential rate of uplift $\Delta\dot{\zeta}^{p}_{AB}(t)$ at the two sites (A, B) on a lake is predicted and compared with the observed value $\Delta\dot{\zeta}^{o}_{AB}(t)$. The optimum earth model is then the one for which the quantity

$$\Psi^{*2}_{k} = \frac{1}{N}\sum_{n=1}^{N}\left[\frac{\Delta\dot{\zeta}^{o}_{AB}(t) - \Delta\dot{\zeta}^{p}_{AB}(t)}{\sigma_n}\right]^2 \tag{6}$$

is a minimum, where the summation is over the N lakes for which observations of lake tilt exist. The σ_n^2 is the variance of the observed differential rate of uplift for the nth lake. The accuracy estimates of the resulting earth-model parameters follow from the statistic Φ^{*2}_{k} similarly defined to that in eq. (4).

3.2 A preliminary comparison of model predictions with the sea- and lake-level records

3.2.1 *The sea-level records*

Predictions, based on the optimum earth- and ice-model parameters derived in Paper I, for the mareograph sites are summarized in Table 1. The corresponding earth-model parameters are: $H_1 = 75$ km, $\eta_{um} = 3.6 \times 10^{20}$ Pa s, $\eta_{lm} = 8 \times 10^{21}$ Pa s, and the ice model is SCAN-2. Agreement with the observed values is broadly satisfactory but some of the discrepancies are larger than would be expected from the observational uncertainties alone. In particular, $\Psi^2_k = 4.2$, compared with the expected value of unity. This large value points to scope for further model improvement, as is illustrated when the residuals ε^{o} are plotted as a function of distance from a nominal location for the centre of rebound in the northern Gulf of Bothnia, the residuals being systematically positive for sites near the centre of rebound (Fig. 1a). Thus what these comparisons do suggest is that either the earth-model parameters are not wholly adequate, or that modifications to the ice sheet are required

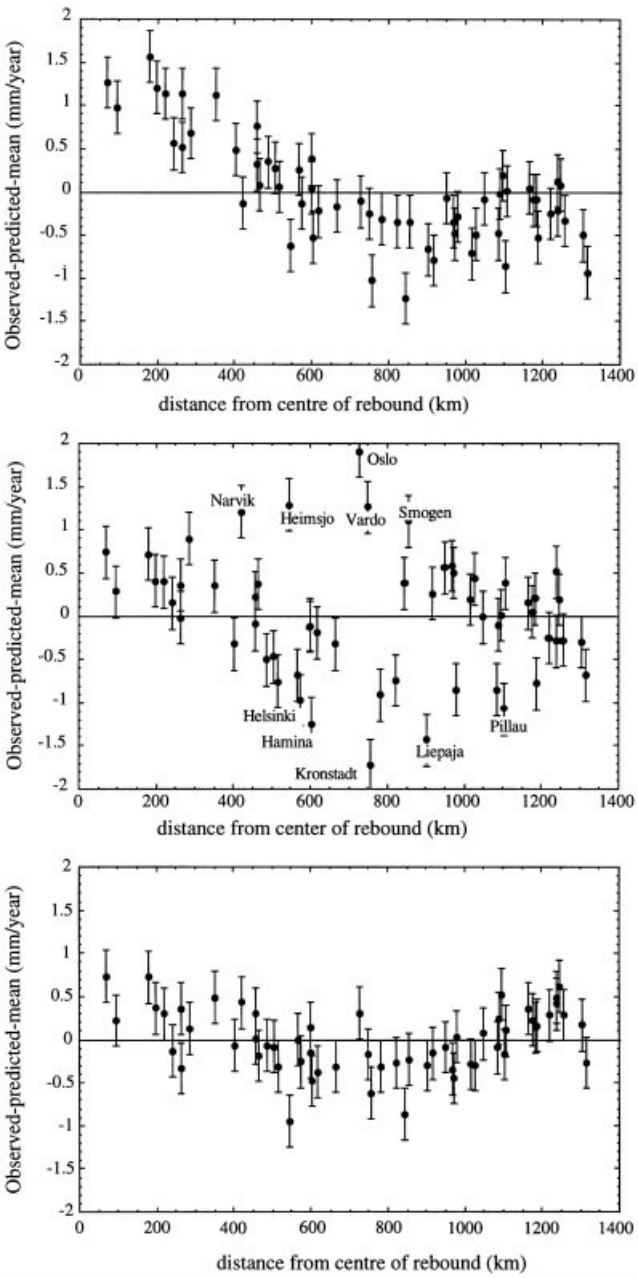

Figure 1. Residuals $\Delta\dot{\zeta}^{o}_{m} - (\Delta\dot{\zeta}^{p,k*}_{m} + \Delta\dot{\zeta}^{e,k*})$ as a function of distance from the centre of the ice load, for (a) the ice model SCAN-2 with the optimum earth-model parameters inferred from the geological evidence, (b) for the ice model SCAN-1 with the earth-model parameters defined by (8a), (c) for the ice model SCAN-2 with the earth-model parameters defined by (11a).

and that it may be possible to use the discrepancies to estimate corrections to either or both sets of parameters.

For this model $\Delta\dot{\zeta}^{e} = -0.95 \pm 0.08$ mm yr^{-1} (standard deviation of the mean), a value representing the average rise in sea level for the past century inferred from all the sea-level monitoring sites. Nine sites lie within the limits defined by (5), as is illustrated in Fig. 2(a) for the southwestern region of Denmark, southern Sweden and the German Baltic coast, and for these records the mean value for the observed secular change is -1.16 ± 0.11 mm yr^{-1}. This result is statistically consistent with that obtained from the total mareograph

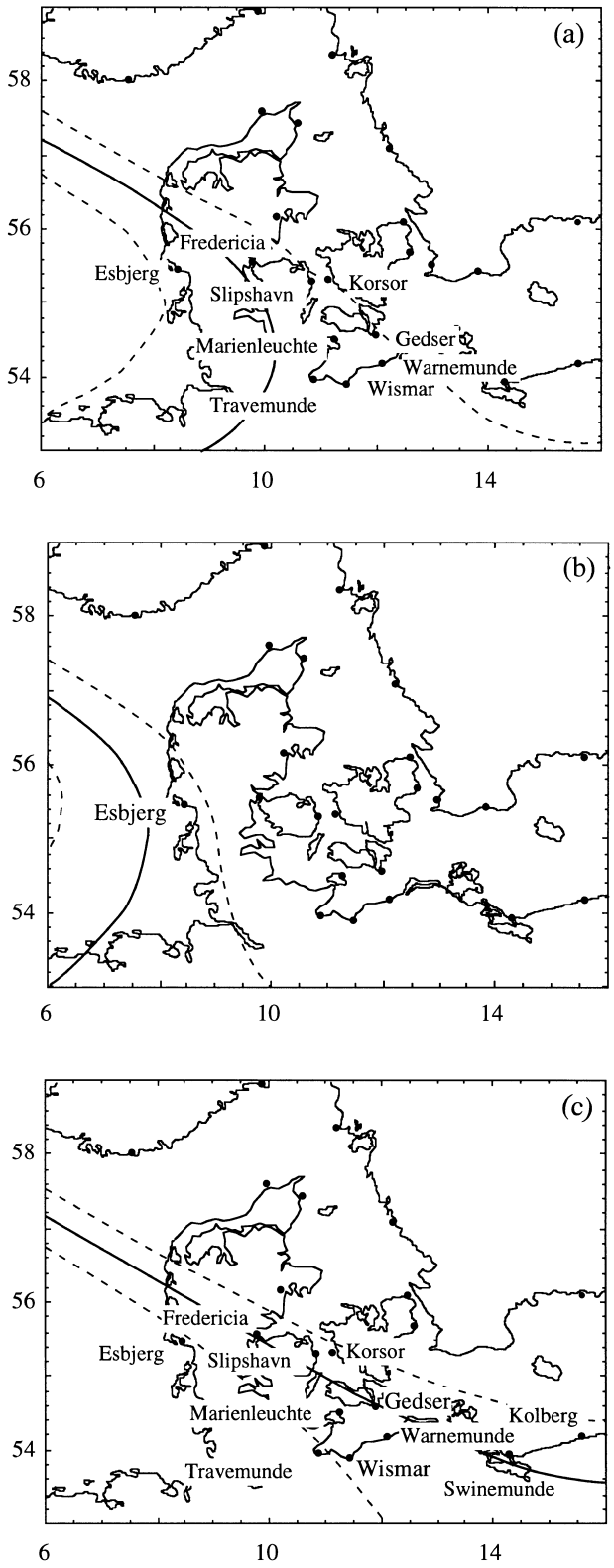

Figure 2. Predicted contours for the zero (solid line) and $\pm\sigma_m$ relative sea-level change (dashed line) for (a) the optimum ice-earth model inferred from the geological evidence for Scandinavia with $\sigma_m = 0.3$ mm yr^{-1}, (b) the solution (8) corresponding to the SCAN-1 ice model, and (c) the solution (11) corresponding to the SCAN-2 ice model. The mareograph sites lying within the limits $\pm\sigma_m$ are identified in each of the three cases, except that in (c) the site of Pillau (in the Gulf of Gdansk) is not shown.

record, suggesting that the choice of earth and ice model does give a satisfactory representation of the long-wavelength part of the rebound signal.

3.2.2 *The lake-level records*

Predictions of the present differential rate of uplift of the four lakes are given in Table 2 for the optimum earth–ice model parameters used above. (The differential rates are defined as the difference in uplift rates between the lake site closest to the centre of rebound less the rate for the site farthest from the rebound centre.) Agreement with the observed values is generally satisfactory with the differences being, with the exception of the Vättern result, less than the nominal observational accuracy discussed above for the observed rates. Nevertheless, for this exception, as well as the two Finnish lakes, the model predictions are less than the observed values, suggesting that a better agreement with the observations may be achievable by modifying either the earth- or ice-model parameters.

3.2.3 *Comment*

Because of the trade-offs that can occur between the various parameters describing the rebound model we do not attempt, in the first instance at least, to seek modifications of the model parameters that were based on the inversion of the geological data. Instead, we first return to the initial ice model SCAN-1, one that is largely free from assumptions about the Earth's response to ice loading, and examine whether or not the essential aspects of the modifications that led to the second model SCAN-2 as well as to the above-used earth-model parameters, are in fact supported by the instrumented sea-level and lake-level data for present-day rates of change.

3.3 Results for ice model SCAN-1

3.3.1 *The sea-level records*

For any earth model E_k the predictions $\Delta\dot{\zeta}^{\mathrm{p}}(\phi, E_k, I_j)$ are compared with the observed values to evaluate the statistic Ψ_k^2 (eq. 3) and a search is conducted throughout the parameter space E_k defined by

$$\left.\begin{aligned} &30 < H_1 < 150 \text{ km} \\ &10^{20} < \eta_{\mathrm{um}} < 10^{21} \text{ Pa s} \\ &10^{21} < \eta_{\mathrm{lm}} < 3 \times 10^{22} \text{ Pa s} \end{aligned}\right\} \qquad (7)$$

to locate the model $E_k(H_1, \eta_{\mathrm{um}}, \eta_{\mathrm{lm}})$ that yields the minimum variance Ψ_k^2. Fig. 3(a) illustrates typical results for the subspace $H_1 = 80$ km and the other parameters within the limits defined by (7). The range of acceptable models, defined by eq. (4) with $\Phi_k^2 = 1.78$, is superimposed upon these results. Resolution for the lower-mantle viscosity from this kind of data is low and models within the range $(2 \times 10^{21} > \eta_{\mathrm{lm}} > 3 \times 10^{22})$ Pa s give essentially the same estimate for Ψ_k^2. Hence a more useful portrayal of the results is in $H_1 - \eta_{\mathrm{um}}$ space as in Fig. 3(b). The mantle parameters for the least variance solution are

$$\begin{aligned} &H_1 = 70 \pm 20 \text{ km}, \\ &\eta_{\mathrm{um}} = (3 \pm 0.5) \times 10^{20} \text{ Pa s}, \\ &\eta_{\mathrm{lm}} \simeq 2 \times 10^{22} \text{ Pa s}, \end{aligned} \qquad (8a)$$

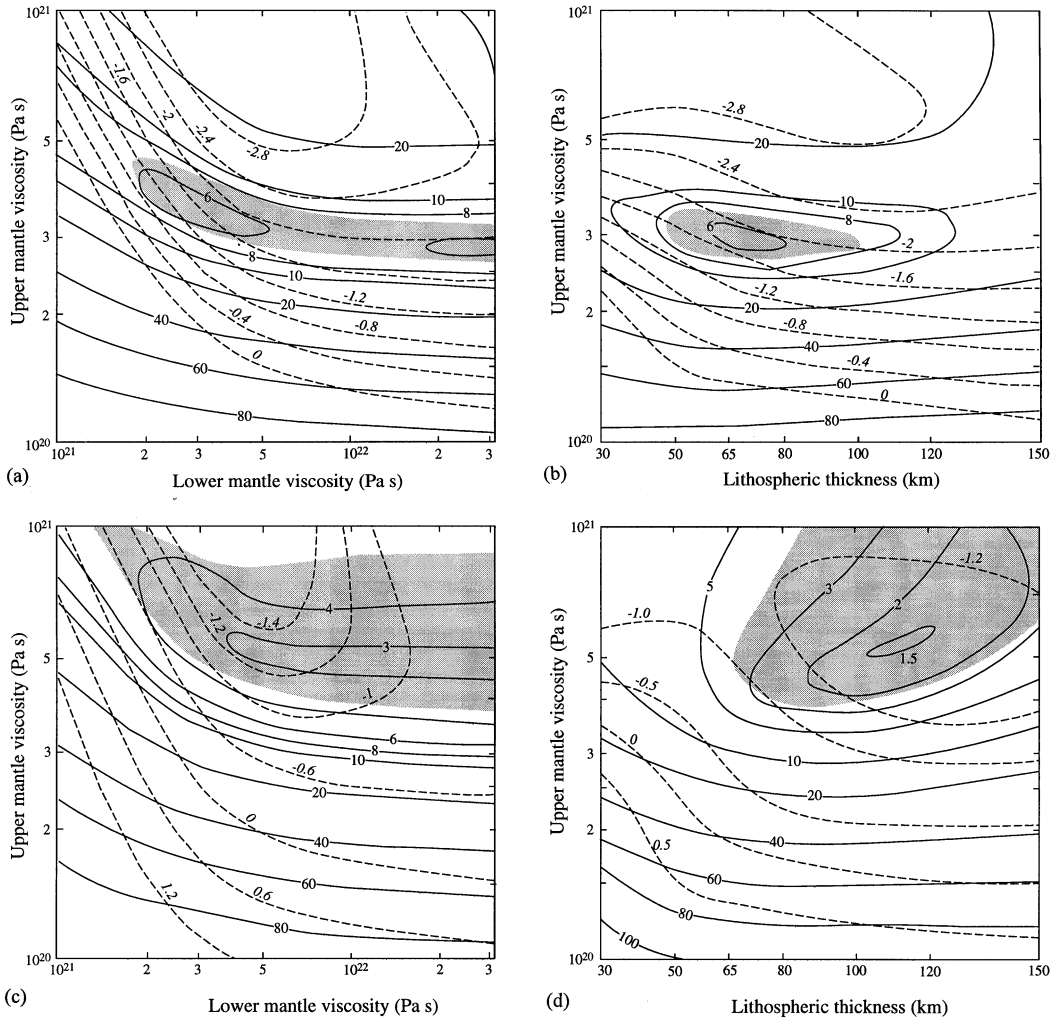

Figure 3. Variance factor Ψ_k^2 (solid lines) and eustatic correction (dashed curves) as a function of (a, c) upper- and lower-mantle viscosity for $H_1 = 80$ km, and (b, d) upper-mantle viscosity and lithospheric thickness for a lower-mantle viscosity of 10^{22} Pa s. The solution space defined by $\Phi_k^2 \leq 1.78$ is shown by the shaded area. The solutions (a, b) correspond to the ice model SCAN-1 and the solutions (c, d) correspond to the ice model SCAN-2.

with

$$\Psi^2_{\min} = 5.3 \tag{8b}$$

and

$$\Delta\dot{\zeta}^{e} = -1.8 \pm 0.7 \text{ mm yr}^{-1}. \tag{8c}$$

The error estimate given in (8c) is now the standard deviation of a single observation. The least-variance estimate is much larger than the expected value of unity, implying that, in the absence of any model errors, the average accuracy of the mareograph record is about $0.3 \times \sqrt{5.3}$ mm yr^{-1}, significantly greater than the analyses of any individual record would suggest. The unsatisfactory aspect of this solution is also illustrated in Fig. 1(b), where the range of the residuals is very much greater than for the case discussed in the previous section (*cf.* Fig. 1a). In particular, the observations from southern Finland and the southeastern shore of the Baltic Sea result in strongly negative residuals (e.g. Kronstadt, Hamina, Helsinki, Liepaja, Pillau), whereas observations from western and northwestern sites (Vardø, Narvik, Heimsjø) and the Oslofjord (Smögen, Oslo) yield primarily positive anomalies (see also Table 1). Within the underlying assumption of spatially uniform earth-model parameters, these residuals point to the ice load being excessive in the east and south and insufficient for central and northwestern Norway as well as to the north and east of the Oslo Fjord region. That is, the residuals point to the inadequacy of scaling the nominal SCAN-1 ice model with a single parameter, and a spatially variable parameter appears warranted: one in which the scale parameter exceeds the average of 0.62 in the northwest and is less than this value in the south and east.

The estimate (8c) for the secular eustatic sea-level rise represents the average value for the 100 year interval from 1892 to 1991 and lies near the upper limit of most estimates inferred from global analyses for a similar time interval (e.g. Gornitz *et al.* 1982; Barnett 1983; Nakiboglu & Lambeck 1991). For the 'best-estimate' earth model (8a), as for a range of models within $\Phi_k^2 = 1.78$, the zero contour for $\Delta\dot{\zeta}^{o}$ generally lies outside the mareograph network examined here (Fig. 2b), and the only site for which the condition (5) is satisfied is Esbjerg, for which $\Delta\dot{\zeta}^{e} = -1.04 \pm 0.3$ mm yr^{-1}.

The use of only a single station to define the secular sea-level change is a questionable practice and is done here only

to determine whether there is a significant trade-off between the rheological parameters and this quantity. A repeat of the model-parameter estimation process, but in which the eustatic rate is now set to this above 'observed' value, leads to

$$H_1 = 80\begin{pmatrix}+20\\-30\end{pmatrix}\text{km},$$

$$\eta_{\rm um} = (3.5 \pm 0.5)\times 10^{20}\ \text{Pa s}, \tag{9a}$$

$$\eta_{\rm lm} = 3\begin{pmatrix}+2\\-1\end{pmatrix}\times 10^{21}\ \text{Pa s},$$

with

$$\Psi^2_{\rm min} = 7.3. \tag{9b}$$

The solution for H_1 and $\eta_{\rm um}$ is similar to that obtained before (8a) but the lower-mantle viscosity estimate is now reduced, in keeping with the trade-off that occurs between $\Delta\dot{\zeta}^{\rm e}$ and those earth-model parameters that dominate the long-wavelength response in the rebound signal, in this case the lower-mantle viscosity. However, for this model the Ψ^2_k is even larger and the solution overall is unsatisfactory.

3.3.2 *The lake-level records*

The analysis of the lake-level data is carried out in a similar manner, with the search conducted through the parameter space (7) for the earth model that leads to a minimum for the statistic defined by (6). Fig. 4 illustrates the results for the four lakes for the SCAN-1 ice model, first for the $\eta_{\rm um} - \eta_{\rm lm}$ space with $H_1 = 80$ km (Fig. 4a), and second for $H_1 - \eta_{\rm um}$ space with $\eta_{\rm lm} = 10^{22}$ Pa s (Fig. 4b). As for the instrumented sea-level data, the resolution for H_1 and $\eta_{\rm lm}$ is poor and the best-resolved parameter is $\eta_{\rm um}$. Overall, the four lake records point to

$$\left.\begin{aligned} H_1 &= 100 \pm 50\ \text{km}\\ \eta_{\rm um} &= 4\begin{pmatrix}+6\\-1\end{pmatrix}\times 10^{20}\ \text{Pa s},\end{aligned}\right\} \tag{10a}$$

with

$$\Psi^2_{\rm min} \simeq 3.6. \tag{10b}$$

This least variance is again relatively high, implying, in the absence of model errors, an observational accuracy of about

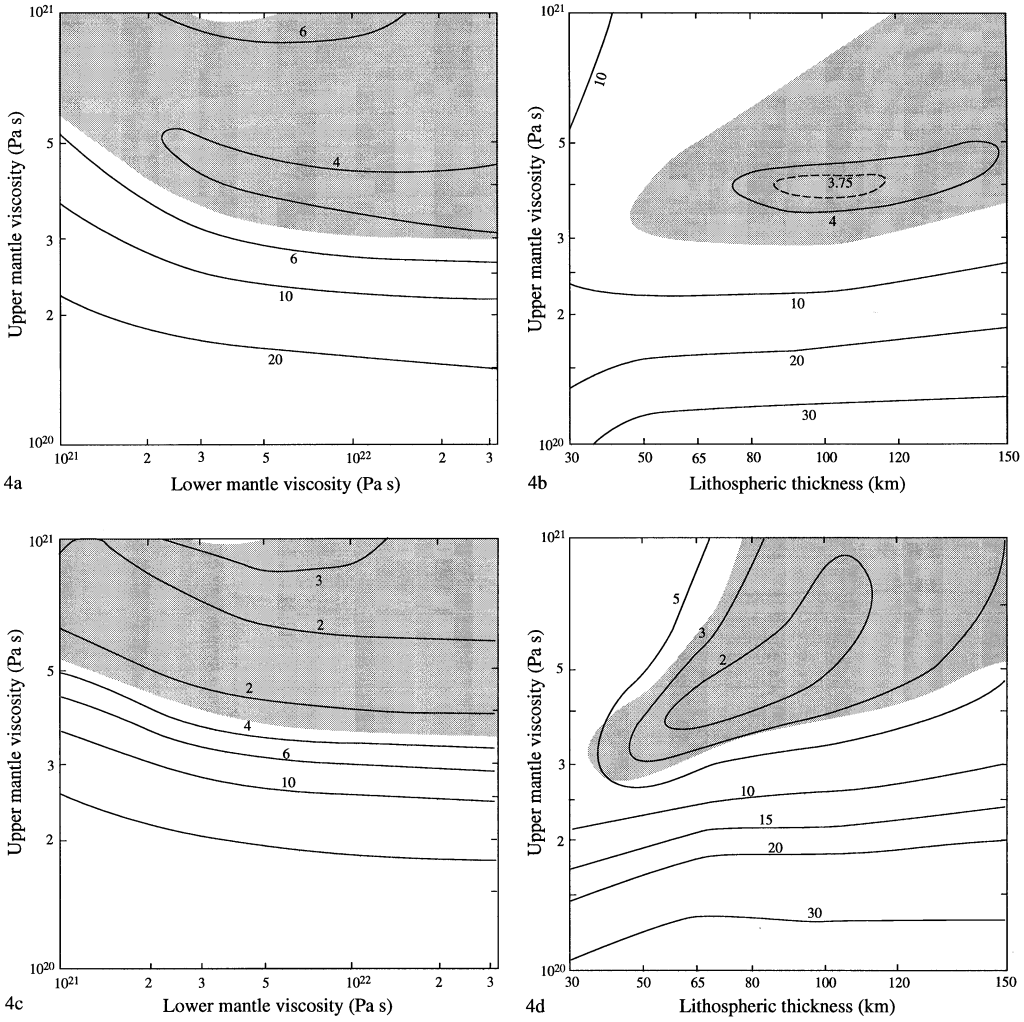

Figure 4. Variance factor Ψ^{*2}_k (eq. 6) for the differential uplift rates across the four lakes: solutions (a, b) correspond to the ice model SCAN-1, and (c, d) correspond to the ice model SCAN-2. Figs (a, c) illustrate the solution in the $\eta_{\rm um}$–$\eta_{\rm lm}$ subspace with $H_1 = 80$ km, and (c, d) illustrate the solution in the H_1–$\eta_{\rm um}$ subspace with $\eta_{\rm lm} = 10^{22}$ Pa s.

$0.2 \times \sqrt{3.6}$ mm yr^{-1} for the rates of lake tilting, at least twice that indicated by the observational data itself.

3.3.3 Comment

The two solutions based on the SCAN-1 ice model give similar results for the rheological parameters defining the three-layered mantle model. In both cases, the lower-mantle viscosity is poorly resolved but appears to be greater than about 5×10^{21} Pa s. In contrast, the average, effective, upper-mantle viscosity is better constrained, at around $(3\text{–}4) \times 10^{20}$ Pa s. Both solutions also rule out models with thin effective lithospheres (< 50 km), and the sea-level monitors do not favour thick-lithosphere models either (Fig. 3b). However, for both data sets, the estimates of the least variance are high, indicating that further refinement of the models is warranted. In particular, in both cases the residuals between observed and predicted values, the latter based on the best-fitting model for the particular data set, are suggestive of a need to modify the ice sheet in a similar way: a reduction of ice thickness over Finland and the Baltic Sea and an increase in ice height over Norway. These modifications are consistent with those inferred from the geological evidence (Paper I) and which led to the ice model SCAN-2. Thus the above analysis is repeated for this second ice model to establish whether the SCAN-2 model indeed yields an improved agreement with the sea- and lake-level data.

3.4 Results for ice model SCAN-2

3.4.1 The sea-level records

Results for the earth-model parameter space and the sea-level analysis are illustrated in Figs 3(c)–(d). The optimum solution for the mantle parameters is now

$$H_1 = 110 \pm 25 \text{ km},$$

$$\eta_{\text{um}} = 5 \begin{pmatrix} +5 \\ -1 \end{pmatrix} \times 10^{20} \text{ Pa s}, \tag{11a}$$

$$\eta_{\text{lm}} \simeq (2 \pm 1) \times 10^{22} \text{ Pa s},$$

with

$$\Psi^2_{\text{min}} \simeq 1.5, \tag{11b}$$

and

$$\Delta\dot{\zeta}^{\text{e}} = -1.05 \pm 0.25 \text{ mm yr}^{-1}. \tag{11c}$$

Again, the resolution for η_{lm} is poor and the principal trade-off that occurs between the model parameters within the neighbourhood of the solution (11) is between this parameter and $\Delta\dot{\zeta}^{\text{e}}$: a reduced value for η_{lm} leading to an increase in the magnitude of $\Delta\dot{\zeta}^{\text{e}}$ (Fig. 3c). The results (11) point to values for both H_1 and η_{um} that are somewhat higher than obtained previously for the SCAN-1 model. However, the least-variance estimate is now much closer to the expected value of unity. Also, the residuals in this case are substantially smaller than for the earlier ice model although they still exhibit some systematic patterns, remaining predominantly positive for sites close to the centre of the ice load (e.g. Pietarsaari in northern Finland) as well as for sites in Denmark and the western Baltic Sea (e.g. Marienleuchte in the Mecklenburger Bucht) (Fig. 1c; Table 1). No model in the parameter space defined by $\Phi^2_k \leq 1.78$ results in residuals that do not exhibit such a pattern, and the results may indicate that in the derivation of the SCAN-2 ice model the reduction in ice height over the central Gulf of Bothnia, as well as over the southern margin, may have been excessive.

The estimate of the eustatic sea-level rise for this model, without any *a priori* constraints on its value, is -1.05 ± 0.25 mm yr^{-1} for the past 100 years, similar to that indicated by the global tide-gauge analyses covering a comparable time span. For the earth-model parameters (11a), the zone of predicted sea levels satisfying (5) passes through central Jylland, southern Sjaelland and along the Baltic coast of Germany to as far east as the Gulf of Gdansk (Fig. 2c) and contains 12 mareograph records whose average observed rate of change is -0.95 ± 0.25 mm yr^{-1}. Relaxing the criterion (5) to $0 \pm 2\sigma_m$ yields essentially the same result.

3.4.2 The lake data

The re-analysis of the lake-tilt data using the SCAN-2 ice model leads to the results (Figs 4c and d)

$$H_1 = 80 \begin{pmatrix} +70 \\ -20 \end{pmatrix} \text{km},$$

$$\eta_{\text{um}} = 4.5 \begin{pmatrix} +5 \\ -1.0 \end{pmatrix} \times 10^{20} \text{ Pa s}, \tag{12a}$$

with

$$\Psi^2_{\text{min}} \simeq 1.5. \tag{12b}$$

As for the sea-level analysis, the SCAN-2 model yields a more reasonable fit to the data than does the SCAN-1 model but the resolution for η_{lm} remains poor.

3.4.3 Comment

Generally, the two analyses based on the SCAN-2 model yield better results than the comparable analyses based on the SCAN-1 model. In particular, the least-variance estimates for both data sets are much reduced for the SCAN-2 model, implying, in the absence of any model errors, that the observed sea-level rates have an average accuracy of about 0.36 mm yr^{-1} and that the average standard deviation of the observed lake tilts is about 0.24 mm yr^{-1}. In both cases, some pattern to the residuals remains, suggesting that further modifications of the ice model could be appropriate but, because of the ever-present risk of magnifying any trade-off between earth-model and ice-model parameters, a further iteration for the ice-sheet modifications is not warranted at this stage.

4 DISCUSSION

For the ice model SCAN-1, the two data sets, the sea-level records and the differential rates of lake-level change, yield similar solutions for the earth-model parameters (Table 3), as do the comparable solutions based on the SCAN-2 data. Thus the interpretation of the two data types in terms of rebound associated with the last deglaciation (in addition to, in the case of the sea-level records, a eustatic rise in sea level) appears to be at least internally consistent. Both ice models lead to similar results for the effective rheological parameters for the upper mantle: an effective lithospheric thickness of between 65

Table 3. Summary of solutions for earth-model parameters and secular rates of sea-level change. Solution number refers to the equation number in the text. The estimate for the eustatic sea level corresponding to the lake-level results (model 12) is inferred from the mareograph records for the coastal sites corrected for the isostatic contributions based on the lake-level derived earth model.

Data type and model constraint	Solution number	Ice sheet	H_1 (km)	η_{um} ($\times 10^{20}$ Pa s)	Ψ_k^2	$\Delta\dot{\zeta}^e$ (mm yr^{-1})
sea level (free $\Delta\dot{\zeta}^e$)	(8)	SCAN-1	70 ± 20	3 ± 0.5	5.3	-1.8 ± 0.3
sea level (fixed $\Delta\dot{\zeta}^e$)	(9)	SCAN-1	$80\begin{pmatrix}+20\\-30\end{pmatrix}$	3.5 ± 0.5	7.3	-1.04 ± 0.3
lake level	(10)	SCAN-1	100 ± 50	$4\begin{pmatrix}\pm 6\\-1\end{pmatrix}$	3.6	
sea level (free $\Delta\dot{\zeta}^e$)	(11)	SCAN-2	110 ± 35	$5\begin{pmatrix}\pm 5\\-1\end{pmatrix}$	1.5	-1.1 ± 0.2
lake level	(12)	SCAN-2	$80\begin{pmatrix}+70\\-20\end{pmatrix}$	$4.5\begin{pmatrix}+5\\-1\end{pmatrix}$	1.5	-1.01 ± 0.2

and 110 km and an effective upper-mantle viscosity of between 3×10^{20} and 5×10^{20} Pa s. In both instances the lower-mantle viscosity is less well constrained. This similarity suggests that, within the resolution of the data, the solution for the earth-model parameters is not strongly dependent on the details of the ice sheet, provided that the volumes and main characteristics of the melting rates are similar. This was not the case for the analysis of the geological data, where a much stronger correlation between the ice- and earth-model parameters was found (Paper I). In this latter case the observational record extends back into late glacial times, where the sea-level change is relatively sensitive to details of the early (and least known) stages of the ice models. Hence a more suitable strategy for future iterations of rebound analyses may be to use the recent observational evidence to constrain the earth-model parameters and to then use the earlier part of the record to constrain the ice-model parameters.

Despite the fact that both ice models lead to similar conclusions about the Earth's effective rheology, SCAN-2 yields the better agreement with the instrumental sea-level and lake-level observations, in terms of both the overall statistical fit of the models to the data (the Ψ_k^2, Ψ_k^{*2}) and the pattern of the residuals

$$\Delta\dot{\zeta}_m^o - (\Delta\dot{\zeta}_m^{p,k*} + \Delta\dot{\zeta}^{e,k*})$$

across the region. This ice model must therefore be the preferred one. In particular, the comparisons of the residuals for the two ice models confirm the essential characteristic inferred from the geological solutions: that ice thickness in the south and east of the ice sheet is significantly less than what is usually assumed to be the case in models where the thickness is characterized by parabolic profiles (see Paper I).

As noted above, the two instrumental records give consistent results for the earth-model parameters within the accuracy estimates of the parameters (Fig. 5), although the lower-mantle viscosity is essentially unconstrained. These solutions are also consistent with the geologically based estimate obtained in Paper I (see Fig. 5), and there appear to be no incompatibilities between the interpretations of the geological data and the modern mareograph records. However, despite the generally good agreement between the model predictions and the observations, some systematic patterns remain in the residuals, as

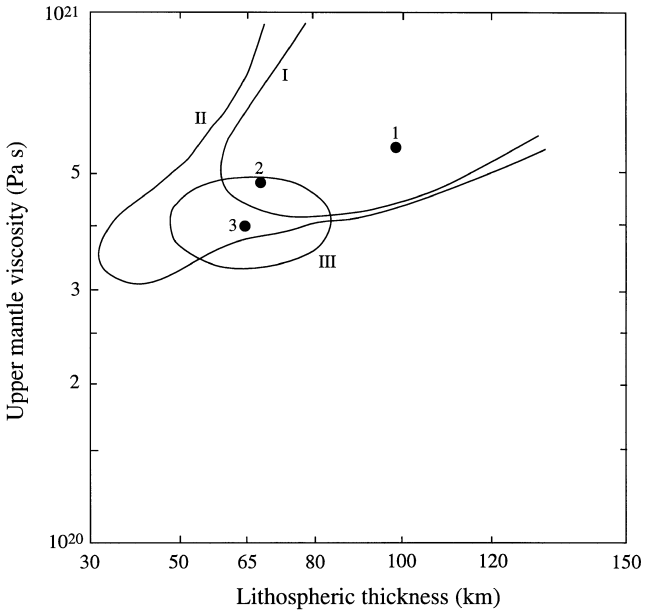

Figure 5. Summary of effective upper mantle parameters based on (1) the modern sea-level record, (2) the modern lake-level records, and (3) the geological record (from Paper I). The lines I and II define the limits of the acceptable solution space, defined by $\Phi_k^2 \leq 1.78$, for the solutions 1 and 2, respectively. The error ellipse III defines the accuracy estimates for solution 3.

can be seen in Fig. 1(c) but more clearly in Fig. 6 for solution (11). In the northern and western parts of the Gulf of Bothnia, for example, the residuals tend to be mainly positive. For southwestern Norway, in contrast, the residuals are negative, as is also the case for central-eastern Sweden, including Gotland and Åland. The pattern of these residuals is different from what one would expect if they were the result of erroneous earth-model parameters (compare Fig. 6 with Fig. 13 of Paper I, for example), and the results suggest that some modifications of the ice sheet SCAN-2 may be appropriate. For example, an increase in the ice heights over northern Finland by about 10 per cent removes the discrepancy observed in Fig. 6. Such an adjustment is small when compared with the differences

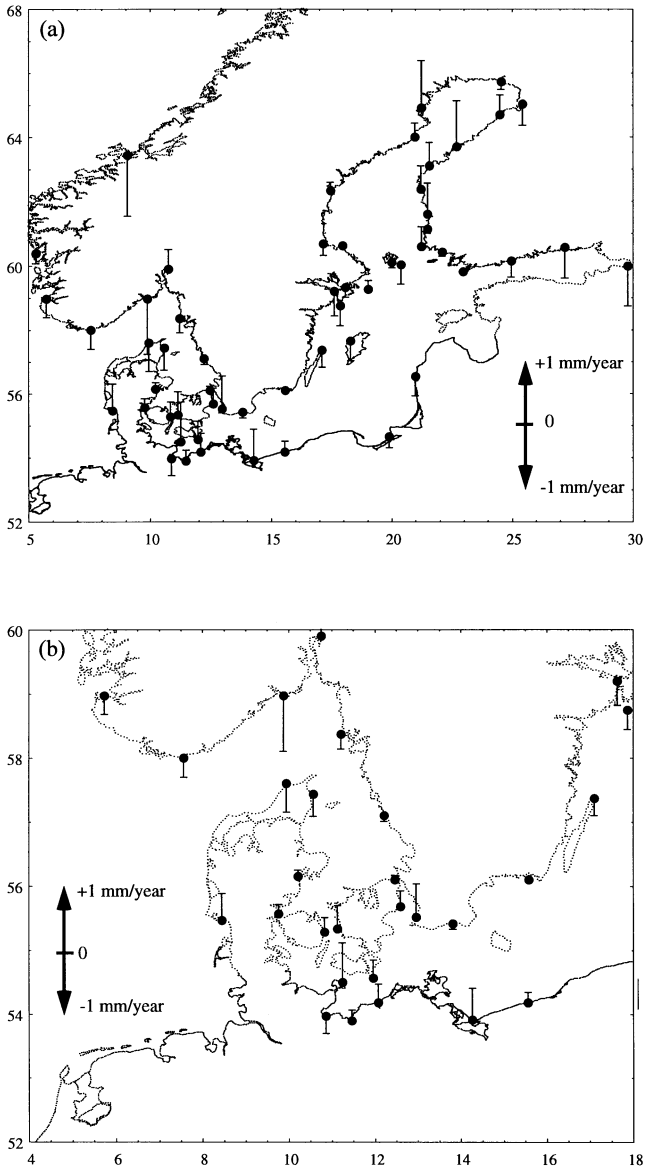

Figure 6. Spatial distribution of the residuals $\Delta\dot{\zeta}^{o}_{sm} - (\Delta\dot{\zeta}^{p,k*}_{m} + \Delta\dot{\zeta}^{e,k*})$ for the ice model SCAN-2 and the earth model defined by (11). (a) For Fennoscandinavia and the southern Baltic region, (b) for Denmark, the western Baltic Sea, and southern Sweden.

between the models SCAN-1 and SCAN-2 and does not vitiate the general arguments for the substantial reduction in ice volumes in the eastern and southern parts of the SCAN-1 ice sheet. A decrease of the SCAN-2 ice heights, also of about 10 per cent, over the southeastern region would remove much of the discrepancy observed there and reinforces the essential characteristic of the SCAN-2 ice model. The residuals over Denmark show a more complex pattern (Fig. 6b), one that cannot be readily interpreted in terms of an adjustment of the ice sheet by a single ice-height scaling parameter. A small reduction in ice height over this area and southern Sweden, of 5–10 per cent, leads to smaller overall residuals but the pattern of alternating signs from north to south across Denmark and Schleswig-Holstein, for example, remains, and the simple strategy of scaling the ice sheets by a single parameter here is not adequate. The geological data discussed in Paper I for Denmark also are not well matched by the predictions, and models with a more realistic description of the ice movements over Denmark need to be explored (Lambeck *et al.* 1997).

An alternative estimate for the secular eustatic sea-level change over the past 100 years follows from the observations for the sites where the condition (5) is satisfied for the earth-model solution (11) as $\Delta\dot{\zeta}^{e} = -0.95 \pm 0.25$ mm yr^{-1}. (As before, the negative sign implies an increase in ocean volume over this time interval.) As some of the above solutions have indicated, trade-offs may occur between this parameter and those earth-model parameters that yield long-wavelength components in the rebound signal, primarily the lower-mantle viscosity. Over the acceptable solution space defined by the Φ^2 statistic (e.g. Figs 3c and d), however, the estimate of $\Delta\dot{\zeta}^{e}$ remains within the above limits so that this trade-off is unlikely to be significant. In particular, magnitudes greater than about 1.4 mm yr^{-1} appear to be ruled out.

Yet another strategy for estimating the eustatic rate is to use the lake record solutions for the rheological parameters (e.g. solution 12a) and to 'correct' the sea-level records for the isostatic effects using these parameters. This leads to $\Delta\dot{\zeta}^{e} = -1.01 \pm 0.2$ mm yr^{-1} for the ice model SCAN-2, a result that is consistent with the earlier estimates and which illustrates that an effective separation of parameters may have been achieved. However, this solution is based on few observations only, and we adopt the solution (11) or

$$\Delta\dot{\zeta}^{e} = -1.05 \pm 0.25 \text{ mm yr} \qquad (13)$$

as the optimum estimate for the average eustatic sea-level change for the 100 year period 1892–1991.

The above estimate of $\Delta\dot{\zeta}^{e}$ is generally consistent with the analyses of global tide-gauge observations for correspondingly long recording periods, both for the more recent analyses as well as for the classical analyses by, for example Lizitzin (1974) and Fairbridge (1961). In terms of the sign convention used for tide-gauge data, of the more recent analyses Gornitz *et al.* (1982) obtained a rate of 1.2 mm yr^{-1}, Barnett (1983) obtained 1.5 mm yr^{-1} and Nakiboglu & Lambeck (1991) obtained 1.15 ± 0.35 mm yr^{-1}. A wholly independent estimate from the analysis of satellite-orbit accelerations, valid for the past two decades, yielded a comparable rate of 1.5 mm yr^{-1} (Lambeck & Johnston 1998). An exception to this range of estimates is the result by Douglas (1995), who obtained a value of 1.8 ± 0.1 mm yr^{-1} for an average record length of about 80 years. [This difference between the various tide-gauge results reflects the uncertainties that can be introduced into the analysis through the use of different averaging or modelling techniques to reduce the effects of tectonics, glacio-isostasy and long-period oceanographic signals (e.g. Barnett 1984).] Also of interest is the analysis of the entire 210 years of record for Stockholm compiled by Ekman (1988). This record was analysed separately for the first 110 years and for the second interval of 100 years, yielding a difference in the apparent uplift of -1.01 ± 0.30 mm yr^{-1}. In so far as the isostatic rate over 200 years has not changed significantly, the difference, if statistically significant, implies a change in the eustatic rate. However, as this difference also equals the eustatic rate for the past 100 years it implies that before about 1880 this rate was vanishingly small and that the observed rate for the past century is not representative of a longer time interval.

Fig. 7 illustrates the predicted crustal uplift, relative to sea level, for the region of Scandinavia and northwestern Europe.

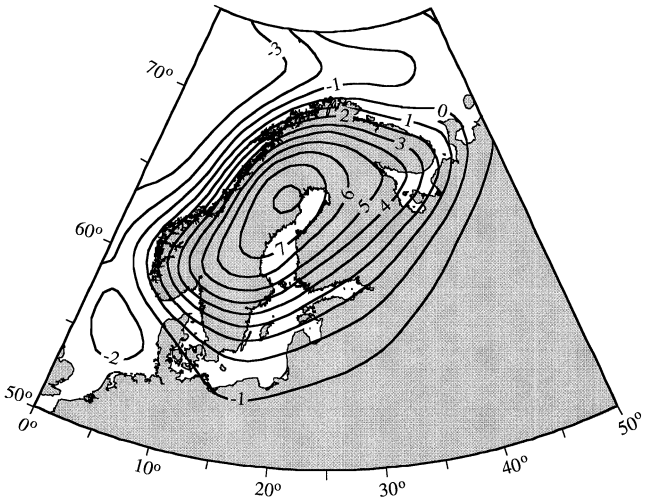

Figure 7. Predicted present-day relative crustal uplift in Scandinavian and northwestern Europe based on solution (11) with the optimum estimate for the eustatic sea-level rise of 1.05 mm yr^{-1}.

These results are based on the SCAN-2 ice model and the solution (11). (Predictions based on solution 12 corresponding to the lake data with $\Delta\dot{\zeta}^{e} = -1.02$ mm yr^{-1} (Table 3) and $\eta_{lm} = 2 \times 10^{22}$ Pa s lead to consistent results and the differences between the two are generally less than the nominal observational accuracies and the larger discrepancies occur in the areas away from the coast where there are no tide-gauge data. This suggests that high precision geodetic levelling for the inland localities may provide further useful constraints on these models.) The predictions illustrated in Fig. 7 can be compared directly with Fig. 3 of Ekman (1996a), which is based on a combination of the mareograph records with repeat geodetic levelling. Overall agreement is satisfactory but some discrepancies remain. The predicted centre of rebound over the Gulf of Bothnia, for example, lies further to the west than the observed centre although the latter is not well defined because of the very limited geodetic data in this area, particularly away from the coast. The other location where some discrepancy occurs is around the White Sea in Russia where the predictions are about 1 mm higher than observed, but here also the geodetic data are sparse and the ice models are not well defined.

5 CONCLUSIONS

The sea- and lake-level records of Fennoscandia and the southern Baltic shore provide important constraints on the mantle response to surface loading, yielding estimates for the effective lithospheric thickness and effective upper-mantle viscosity that are consistent with analyses of geological records of sea-level change for the same region (*cf.* Paper I). The advantage of these instrumental records is that they are homogeneous in data quality, of relatively high accuracy and of good geographical coverage. Also, because the epoch of observation is long after the end of deglaciation, but not so long that the isostatic signal has decayed to a level below the measurement noise, the resulting earth-model parameters are less dependent on the details of ice model than is the case for the geological record, where a significant part of the observational record extends back into Lateglacial times, provided that the bulk characteristics of the ice models are consistent. Thus distinctly different ice models (SCAN-1 and SCAN-2), but with the same ice limits, approximately the same ice volume and comparable overall rates of melting, yield similar solutions for the earth-model parameters. The preferred solution for the effective mantle parameters are given by (11). The effective viscosity of the lower mantle is poorly constrained by these data.

The pattern of the discrepancies between the observations and the model predictions provides useful insights into the spatial distribution of ice within the ice sheet and, in general, these point to ice loads that were proportionally thinner in the east and south than in the northwest and west. These inferences are consistent with those previously drawn from the geological data (Paper 1).

The sea-level records also contain information on the eustatic sea-level change. Some dependence for this quantity on both ice-model and earth-model parameters results unless precautions are taken to avoid the trade-offs between parameters. Two different approaches have been used which lead to solutions that have achieved an effective separation of parameters within the accuracy limits of the solutions. For a given earth model the region can be predicted where the isostatic movement of the crust is zero to within the observational accuracy of the mareograph data. Instrumental records from sites within this region therefore should provide an unbiased estimate of eustatic sea-level change. In a second approach the records of the tilting of the four large lakes in Sweden and Finland have been used to estimate the earth-model parameters, and the corresponding isostatic corrections to the sea-level records are based on these estimates. The resulting eustatic sea-level rises based on these two approaches are consistent although the lake-level solution is much less precise. Also, the eustatic-rate estimates, based on the first approach, are essentially independent of the choice of ice model (compare solutions 9 and 11 of Table 3), although for the SCAN-1 ice model only one site falls within the region for which the predicted isostatic sea-level change is zero to within observational error and the agreement may be fortuitous. The optimum result for the eustatic sea-level rise based on the mareograph records is 1.05 ± 0.25 mm yr^{-1}, a value that represents the average for the past 100 years. The much longer, more than 200 years, Stockholm record indicates that it may not be possible to extrapolate this rate further back in time and that the eustatic rise in sea level may have been lower during the century before about 1880 than for the subsequent century.

ACKNOWLEDGMENTS

This research was partly funded by an International Science and Technology grant from the Commonwealth of Australia, Department of Industry, Science and Tourism.

REFERENCES

Andersen, B.G., 1981. Late Weichselian ice sheets in Eurasia and Greenland, in *The Last Great Ice Sheets,* pp. 1–65, eds Denton, G.H. & Hughes, T.J., J. Wiley, New York.

Barnett, T.P., 1983. Recent changes in sea level and their possible causes, *Climate Change,* **5,** 15–38.

Barnett, T.P., 1984. The estimation of global sea-level change: A problem of uniqueness, *J. geophys. Res.,* **89,** 7980–7988.

Denton, G.H. & Hughes, T.J. (eds), 1981. *The Last Great Ice Sheets,* Wiley, New York.

Douglas, B.C., 1995. Global sea level change—determination and interpretation, *Rev. Geophys.,* **33,** 1425–1432.

Ekman, M., 1988. The world's longest continued series of sea-level observations, *Pure appl. Geophys.,* **127,** 73–77.

Ekman, M., 1996a. A consistent map of the postglacial uplift of Fennoscandia, *Terra Nova,* **8,** 158–165.

Ekman, M., 1996b. A common pattern for interannual and periodical sea-level variations in the Baltic Sea and adjacent waters, *Geophysica,* **32,** 261–272.

Ekman, M., 1997. Anomalous winter climate coupled to extreme annual means in the Baltic Sea level during the last 200 years, *Small Publ. Hist. Geophys.,* **3.**

Fairbridge, R.W., 1961. Eustatic changes in sea level, *Phys. Chem. Earth,* **4,** 99–185.

Gornitz, V., Lebedeff, S. & Hansen, J., 1982. Global sea level trend in the past century, *Science,* **215,** 1611–1614.

Kleman, J., Hättestrand, C., Borgström, I. & Stroeven, A., 1997. Fennoscandian palaeoglaciology reconstructed using a glacial geological inversion model, *J. Glaciol.,* **43,** 283–299.

Lambeck, K. & Johnston, P., 1998. The viscosity of the mantle from analyses of glacial rebound phenomena, in *The Earth's mantle,* pp. 461–502, ed. Jackson, I., Cambridge University Press, Cambridge.

Lambeck, K., Johnston, P. & Nakada, M., 1990. Holocene glacial rebound and sea-level change in NW Europe, *Geophys. J. Int.,* **103,** 451–468.

Lambeck, K., Johnston, P. & Smither, C., 1997. Sea-level change in the North Sea, Rept MDGAP-9769, Part 3, pp. 29–34, Meetkundige Dienst, Rijkswaterstaat, Delft, The Netherlands.

Lambeck, K., Smither, C. & Johnston, P., 1998. Sea-level change, glacial rebound and mantle viscosity for northern Europe, *Geophys. J. Int.,* **134,** 102–144.

Lizitzin, E., 1974. *Sea Level Change,* Elsevier, Amsterdam.

Nakiboglu, S.M. & Lambeck, K., 1991. Secular sea-level change, in *Glacial Isotasy, Sea Level and Mantle Rheology,* pp. 237–258, eds Sabadini, R., Lambeck, K. & Boschi, E., Kluwer, Dordrecht

Paterson, W.S.B., 1969. *The Physics of Glaciers,* Pergamon, New York.

Pedersen, S.S., 1995. Israndslinier i Norden, Danm. geol. Unders., Copenhagen.

Samuelsson, M. & Stigebrandt, A., 1996. Main characteristics of the long-term sea-level variability in the Baltic Sea, *Tellus,* **48,** 672–683.

Sirén, A., 1951. On computing the land uplift from the lake water level records in Finland, *Fennia,* **73** (5), 1–181.

Vermeer, M., Kakkuri, J., Mälkki, P., Boman, H., Kahma, K.K. & Leppäranta, M., 1988. Land uplift and sea level variability spectrum using fully measured monthly means of tide gauge readings, *Finn. Mar Res.,* **256,** 3–75.